

Shear Lag in Reinforced Concrete T-Beams with Web Openings

Dr. Eyad Kadhum Sayhood

Building and Construction Department, University of Technology/ Baghdad
Email: dr_eyad_alhachamee@yahoo.com

Dr. Nisreen Saleh

Building and Construction Department, University of Technology/ Baghdad
Email: nisreen_alnimer@yahoo.com

Ahmed S.Hanon

Building and Construction Department, University of Technology/ Baghdad

Received on:11/1/2016 & Accepted on:21/4/2016

ABSTRACT

In this paper, an extensive study is carried out 18 beams on the behavior of T-beams (8 with web openings, 10 without openings). Compressive strains distribution at the flanged are investigated with the presence of the openings in web to recheck the effective width of flange with real flange width. Parametric study are considered in this paper includes the compressive strength, longitudinal flexural reinforcement, flange reinforcement, shear reinforcement and the web openings (location, shape, size). Generally, standard codes of practice have overestimated effective flange width due to concentrated load effect, and codes do not take into account the web openings effect. Based on the results, the enhancement in effective width for each parameter were 9.1%-13.36%(compressive strength),10.1%-13.3%(longitudinal flexural reinforcement),7.6%-18.2%(flange reinforcement),3.35%-5.7%(shear reinforcement), the web openings reduced the effective flange width by 15% (openings at mid span) and 5% (openings at quarter span) and the circular opening gave an optimum effective width better than rectangular opening were located both at quarter span.

Keywords: Experimental Study, Reinforced T-beams, Web Openings. Effective Flange Width

INTRODUCTION

Reinforced concrete system normally consists of slab and beams that is placed monolithically and as a result T- Beams created and the two parts act together to resist the applied loads. In the construction of modern building, a network of pipes and ducts is necessary to accommodate essential service like water supply, sewage, air-conditioning, electricity, telephone, and the computer network. Usually, pipes and ducts are placed underneath the beam soffit or penetrate horizontally the web beam or vertically the slabs and, for aesthetic reasons, are covered by a suspended ceiling or by special decoration. Since the strength of concrete in tension is considerably lower than its strength in compression design for shear becomes of major importance in all types of concrete structures.

The reduced stiffness of the beam may also give rise to excessive deflection under service load and result in a considerable redistribution of internal forces and moments in a continuous beam unless special reinforcement is provided in sufficient quantity

with proper detailing, the strength and serviceability of such a beam may be seriously affected.

Shear Lag and Effective Flange Width.

The conventional engineering theory of bending assumes that plane sections before cracks remain plane, also after bending which means that shearing strain are neglected. The term shear lag is used to describe the discrepancies between the approximate engineering theory, and the real behavior that results in both the increases in the stresses in the flange component adjacent to the web component in a T-beams, and to the decreases in the stresses in the flange component away from the web as shown in figure (1).^[2]

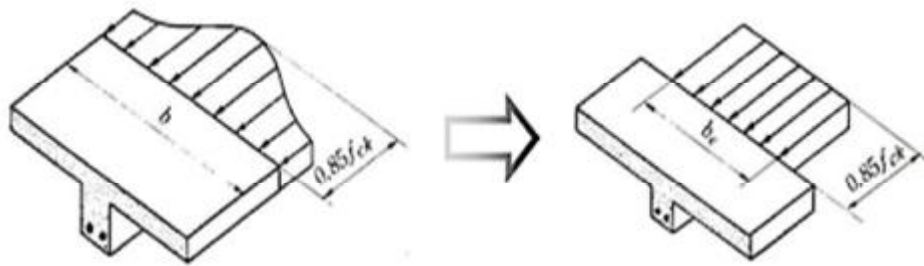


Figure (1) Shear Lag and Effective Width of T-beams

The effective width of a flange is the width of a hypothetical flange that compresses uniformly across its width by the same amount as the loaded edge of the real flange under the same edge shear forces. Alternatively, the effective width can be thought of as the width of theoretical flange which carries a compression force with uniform stress of magnitude equal to the peak stress at the edge of the prototype wide flange when carrying the same total compression force.

Experimental Program

The experimental program consists of testing 18 simply supported beams. Beams test have been carried out to create an understanding of flexural failure for beams by using static one point load at mid span and to try reaching a better understanding of flexural strength for the shallow beams. All beams divided in two groups which have been illustrated into (Group A, Group B), Group A main consider the change in reinforcing parameters (without opening), Group B consider the change in location, size and number of openings (with opening) as shown in table (1), The specimens have been achieved with condition of ACI 318-14 to check the clear span to depth ratio ($L_n / h > 4.0$).

Table (1) Details of Specimens.

Group	Beams	Sup group	L_n (m)	b_w (mm)	b_p (mm)	b_r (mm)	h (mm)	P_{cs}	P_{cs+}	P_{cs+}	f'_c MPa	opening	notes
Group A Without Opening	A1	A11	1.5	180	350	50	350	0.0143989	0.001795	0.001745	21	-	CONT1
		A12	1.5	180	350	50	350	0.0143989	0	0.001745	21	-	CONT2
	A2	A21	1.5	180	350	50	350	0.0143989	0.001795	0.001745	24	-	EFF. OF f'_c
		A22	1.5	180	350	50	350	0.0143989	0.001795	0.001745	30	-	
	A3	A31	1.5	180	350	50	350	0.017998	0.001795	0.001745	21	-	EFF. OF P_w
		A32	1.5	180	350	50	350	0.02498	0.001795	0.001745	21	-	
	A4	A41	1.5	180	350	50	350	0.0143989	0.002693	0.001745	21	-	EFF. OF P_v
		A42	1.5	180	350	50	350	0.0143989	0.003590	0.001745	21	-	
	A5	A51	1.5	180	350	50	350	0.0143989	0.001795	0.002721	21	-	EFF. OF P_v
		A52	1.5	180	350	50	350	0.0143989	0.001795	0.0039269	21	-	
	B1	B11	1.5	180	350	50	350	0.0143989	0.001795	0.001745	21	1SQRF	EFF. OF NO. OF OPENING
		B12	1.5	180	350	50	350	0.0143989	0.001795	0.001745	21	1SQRF	
		B13	1.5	180	350	50	350	0.0143989	0.001795	0.001745	21	3SQRF	
Group B With Opening	B2	B21	1.5	180	350	50	350	0.0143989	0.001795	0.001745	21	1CIR†	EFF. OF SHAPE OF OPENING
		B22	1.5	180	350	50	350	0.0143989	0.001795	0.001745	21	1CIR	
		B23	1.5	180	350	50	350	0.0143989	0.001795	0.001745	21	3CIR	
	B3	B31	1.5	180	350	50	350	0.0143989	0.001795	0.001745	21	1SQRF	SIZE OPENING
		B32	1.5	180	350	50	350	0.0143989	0.001795	0.001745	21	1CIR**	

* Ratio of longitudinal flexural reinforcement.

† One square opening at quarter span with size 100x100 mm.

• One square opening at quarter span with size 150x150 mm.

** Ratio of longitudinal flange reinforcement.

‡ One circle opening at quarter span with size D=100 mm.

•• One circle opening at quarter span with size D=150 mm.

*** Ration of shear reinforcement (Stirrups).

The variables which have been investigated in Group A, included 10 beams where longitudinal reinforcement, flange reinforcement, shear reinforcement, concrete compressive strength, were the main variables in this group. Group B included eight beams and the location, size and number of openings is the main variables in this group. shape, size and location of opening at web were selected away from distance (quarter span = 375 mm, mid span = 750 mm), the dimension of openings are 100x100 and 150x150 mm for square openings, 100 mm and 150 mm diameter for circular openings. All the openings have been located under neutral axis of the concrete beams. Details of reinforcement for T-beams and openings locations are illustrated in figure (2).

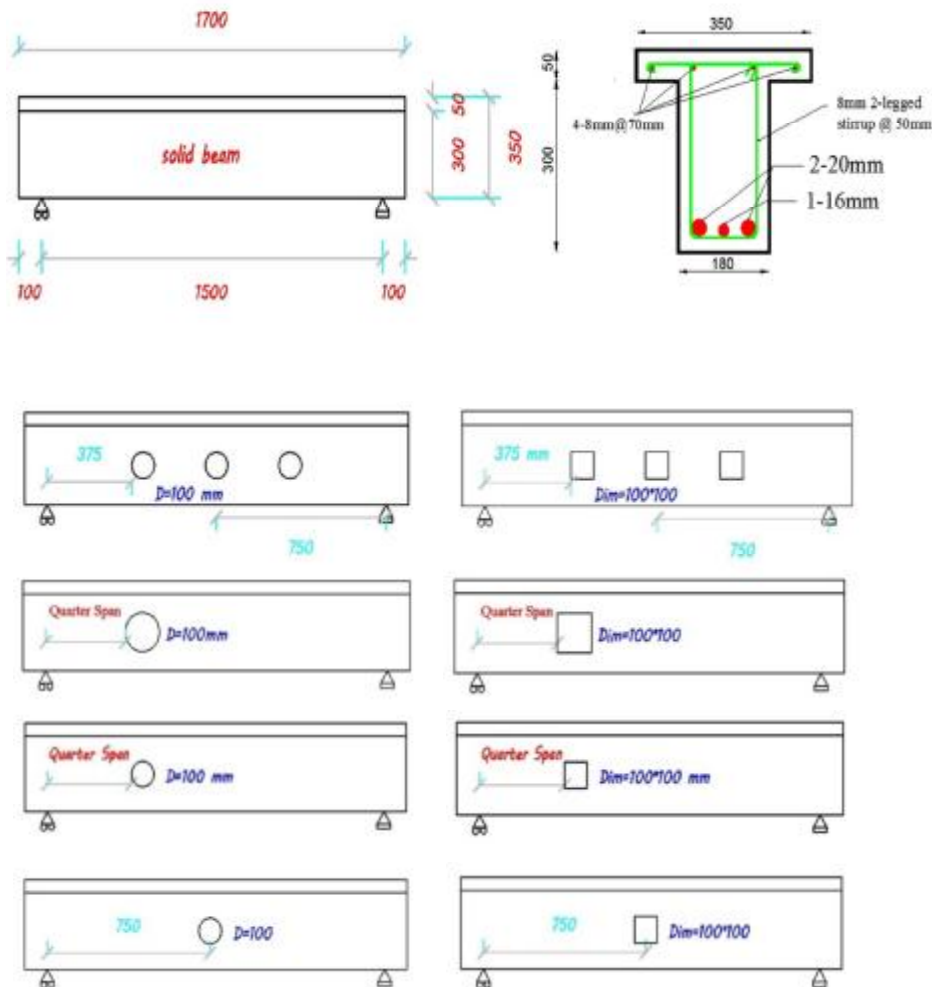


Figure (2) Details of reinforcement and locations of openings

Method of Testing of T-Beams.

All beams and control specimens were removed from curing water at the age 28 days. The beams were cleaned and painted in order to clarify the crack propagation. The demec point positions were located as shown in figure (3), and then mounted on the beams. Each beam was labeled and locations of support points, loading point, and the dial gauge position were marked on the surface to facilitate the precise setup of testing equipment. The beams were placed in the machine on the support with clear span of 1500 mm and adjusted so that the centerline of supports, load arms and dial gauges were fixed at their correct and proper locations. To avoid local failure at load application and support positions and to insure uniform bearing stress at these regions, steel support plates were used of (180 x 100 x 15) mm ,(pinned and roller) these supports are placed so that the center line of the steel support and centerline of load position coincide.

Loading was started by the application of a point load at mid span from the testing machine, initially the zero-load reading for the mechanical deflection gauges as well as the dial gauges was taken and then a load increment of 2 kN was applied and release in order to recheck the zero-load reading.

The load magnitude for each load stage was chosen according to the expected strength of the beams. At each load increment, concrete surface deflection, and strain reading were read and a search was made for the appearance of the cracks and marked on the surface of the beam. The magnitude of the loads stage at which these cracks occurred were read and written. At failure stage, when the beam processes a drop in loading with increasing of deformations, the failure load was recorded, and the load was removed. Some photos were taken to receive the final crack pattern as shown in figure (4).

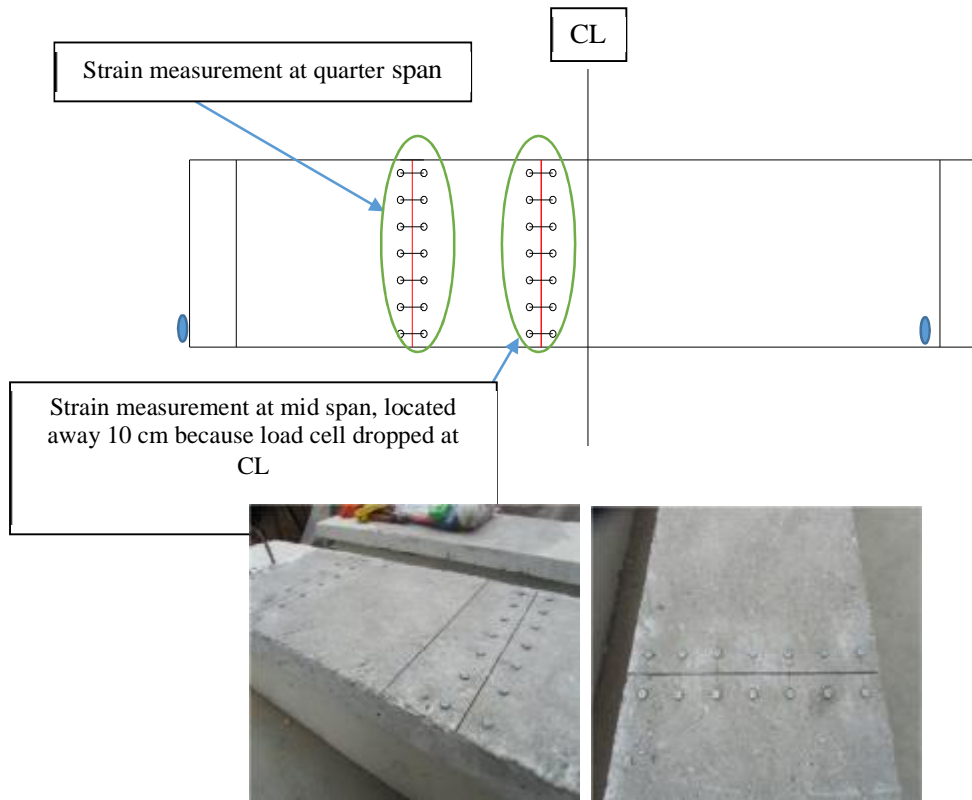


Figure (3) measurement of strain distribution along flange width

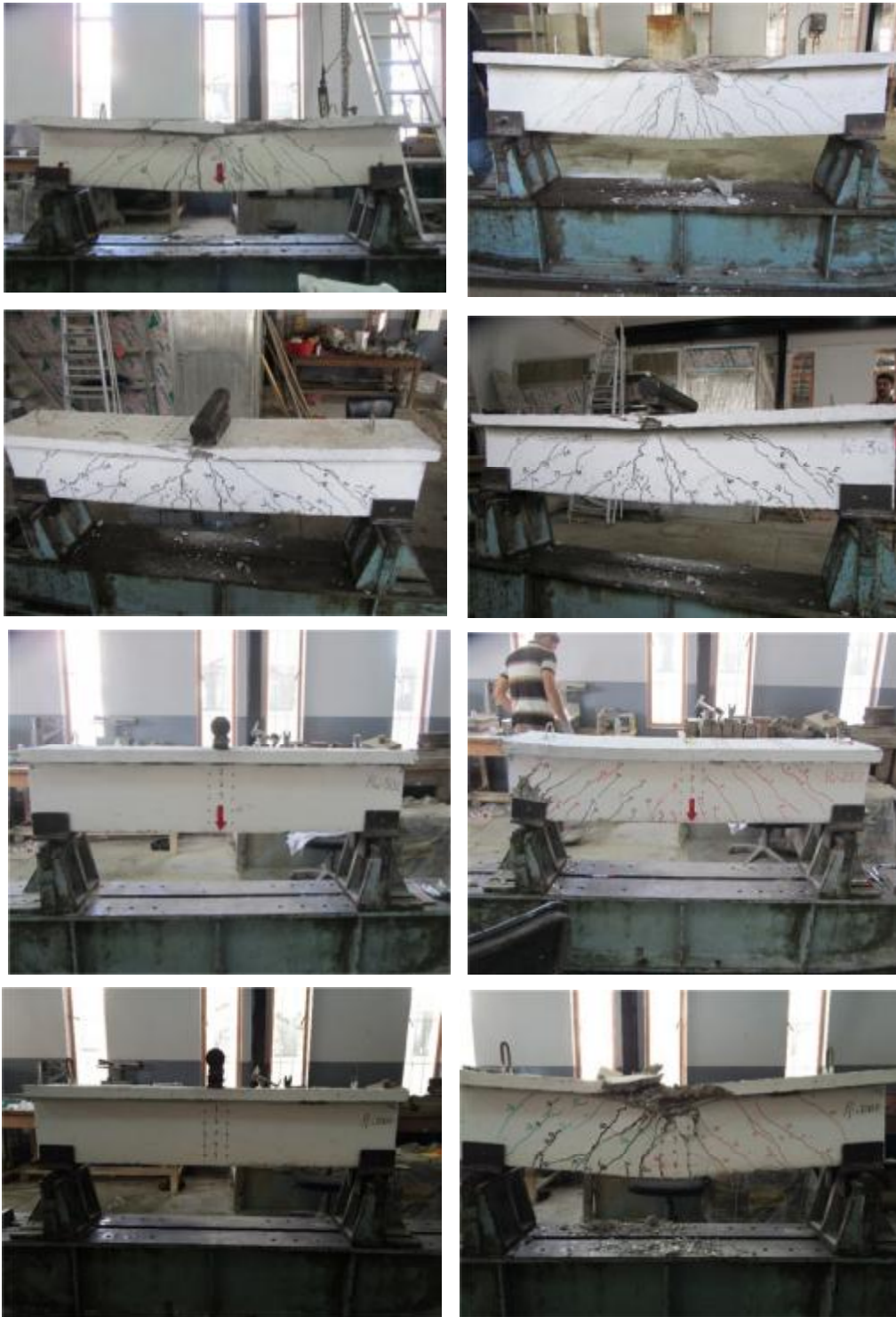


Figure (4) Final crack pattern (continuo)



Figure (4) Final crack pattern

The First Cracking, Ultimate Loading and Calculate The Effective Width.

The control beams have been illustrated in table (2) and namely A11, A12 with reinforcement flange and without reinforcement respectively. The distribution of longitudinal strain on top surface for these beams is shown in figures (6) and (7). Control Beams are tested at the same day and the first beam A11 with flange reinforcement ratio of 0.001795 which contributed with concrete to give suitable strain distribution and effective width closely 61% of real flange width (350 mm), while in the Second beam A12 where no flange reinforcement is provided early crushing stage occurred given of effective flange width 53% of real flange width. Two beams are considered as control beams to compare the other parameters with them.

Figures (8) and (9) show that the increase in compressive strength for beam A21 by 14.29% (21 Mpa to 24 Mpa) causes an increase in the longitudinal strain at mid and quarter span by 16 %, while beam A22 has increase by about 33.45 % in the longitudinal strain at mid and quarter span is illustrated due to an increase in compressive strength by 42.86 % (21 Mpa to 30 Mpa). Also it is observed that when a compressive strength increased to (24 Mpa and 30 Mpa) the effective width of flange increased by 9.1 % and 13.64% respectively.

Figures (10) and (11) show the effect of longitudinal reinforcement at tension zone, it can be seen that increasing the amount of reinforcement results in an increase in the compression block (C) that lead to biggest area for flange longitudinal stresses. Comparing with control beam A11, increasing percentage of steel ratio used in beams A31 and A32 are (25%, 50%) respectively. Increasing in ρ_w increases the tension resistance of the member by increasing the area of reinforcement and hence decreasing the tensile stresses induced in the surrounding concrete. Also, increasing ρ_w effects on the aggregate interlock capacity, beams with low ρ_w will have wide long crack compared to the shorter narrow cracks found in beams with high ρ_w , since the aggregate interlock mechanism depends on the crack width.

Figures (12) and (13) show the beams A41 and A42 have flange steel ratio of (50 % and 100 %) greater than the control beam (A11) respectively. there is an increase in longitudinal strain by (106 %) and (143 %) respectively for the two beams, the effective width of flange increased by 7.6 % for A41 and 18.2% for A42.

Figures (14) and (15) indicate that the strain distributions for three beams are close. The increase in longitudinal strain is 1.62 % and 5.65 % for beams A51 and A52 respectively , while the increase in effective flange width is only (3.35 %, 5.7 %) respectively. It can be concluded that the shear reinforcement has insignificant effect on effective flange width.

Two beams with openings B11 and B21 either rectangular 100x100 mm or circular of 100 diameter located at quarter span (375 mm) from the face of support were tested to investigate the effect of opening shape. Location has been chosen in this position to avoid the maximum moment at mid span. The effect of rectangular and circular opening on longitudinal strain distribution in flange is illustrated in figures (16) and (17). Rectangular opening through the web has four corners around the periphery that leads to concentrate the stresses at corners during service loading. From the obtained results, it can be seen that the suitable shape to give approximately value nearest to the results of beam without opening is the beam with circular opening more than rectangular opening. Effective width ratio (b_e/b_f) of beams B11 and B21 with rectangular or circular opening is (58%, 60%) respectively, compared with control beam A11 (61 % closed with real flange).

To investigate the behavior of beams with different locations of openings and to find the effect on the longitudinal strain distribution along the width of flange, two beams B12 and B22 with one opening (rectangular or circular) at mid span respectively are tested, these openings have the same dimensions of the beams B11, B21 respectively to compare the results of each other, figure (18) and (19) illustrated the longitudinal strain distributions for these beams. Opening at mid span leads to higher deflection than that at quarter span. Also, strain distribution appears in regular shape when the opening away from mid span is shown in

figures. The beam has been weakened at the position of opening specialist at mid span than the quarter and that leads to higher compression strain with small effective width compared with the beams without openings or with opening at quarter point. Effective width ratio (b_e/b_f) of beams B21 and B22 with rectangular or circular opening is (52%, 53%) respectively, compared with control beam A11 (61 % closed with real flange).

When two or more openings are placed closed to each other in a beam (two in each side of quarter and one at the mid span), the strain distribution is not clear. Stresses around opening have been overlapped and rose causing early failure. The figures (20) to (23) show the strain distribution for the beams B13 and B23 and compared with the solid control beam A11. Effective width along the flange is different because the number of opening leads a higher stress at midpoint of flange for each opening and reduced steeper at the sides. This give little area under curve compared with the control beam or beam with one opening. The average effective width equals 182 mm for rectangular openings and 184 for circular openings, approximately 52% and 53% of real flange width respectively.

Making opening with size 150x150 mm and at quarter span for beam B31 and opening 150mm diameter at quarter span for beam B32, caused the cracks to start and quickly propagate at early stage. This is illustrated to great size of opening (1/3 depth of beam) and the stresses are concentrated at corners of openings that leads to shear failure suddenly without records for strain. Eventually it's concluded that if the size of openings bigger than 1/3 depth of the beam, the failure in shear is possible nearest the opening. Both beams with circular or rectangular openings are failed in shear.

The effective flange width may be defined in variety of ways. Figure (5) shows generally a function of the longitudinal strain at the top surface of the flange; so it can be obtained by integration of the rigorously calculated longitudinal strain in the slab at top surface and dividing by the peak value of strain.

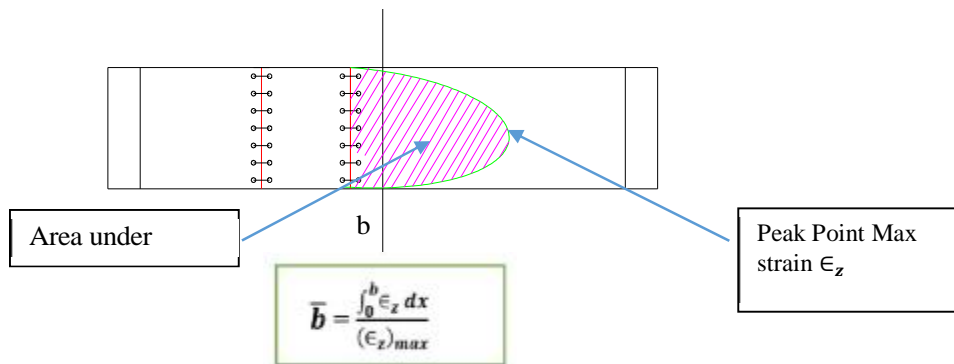


Figure (5) calculation of effective width

Where (\bar{b}) is effective flange width, (b) is a width of flange, (ϵ_z) represent the normal strain in the longitudinal direction, and $((\epsilon_z)_{max})$ is the maximum normal strain (peak strain). This equation is calculated using an approximate method rule (Simpson's rule). The required calculations are done by using EXCEL computer program calculations are done by using EXCEL computer program.

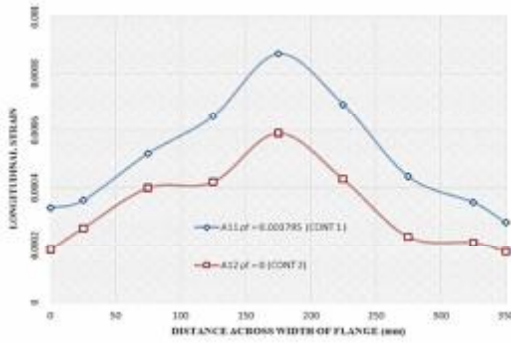


Figure (6) Flange top surface strain distribution at mid span and crack loading for beams A11,A12

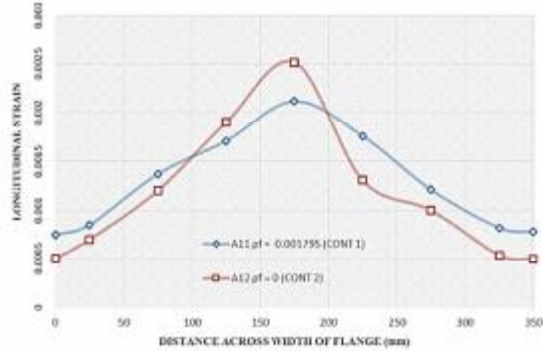


Figure (7) Flange top surface strain distribution at mid span and ultimate loading for beams A11,A12

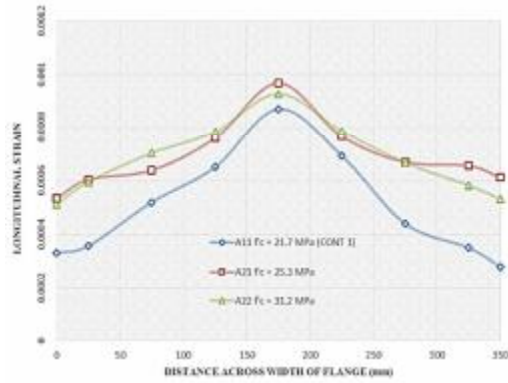


Figure (8) Flange top surface strain distribution at mid span and crack loading for beams A11,A21,A22

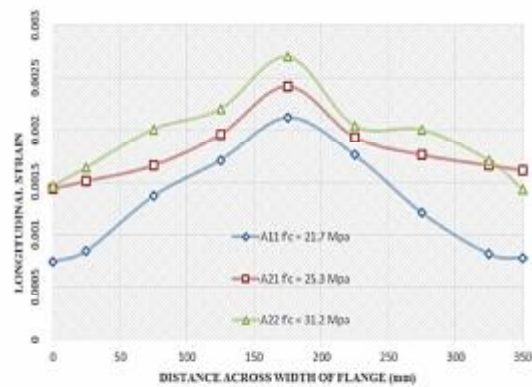


Figure (9) flange top surface strain distribution at mid span and ultimate loading for beams A11,A21,A22

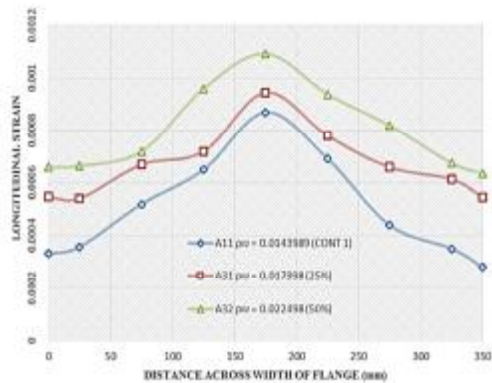


Figure (10) flange top surface strain distribution at mid span and crack loading for beams A11,A31,A32

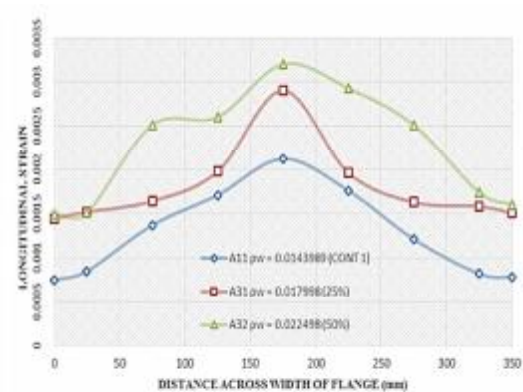


Figure (11) Flange top surface strain distribution at mid span and ultimate loading for beams A11,A31,A32

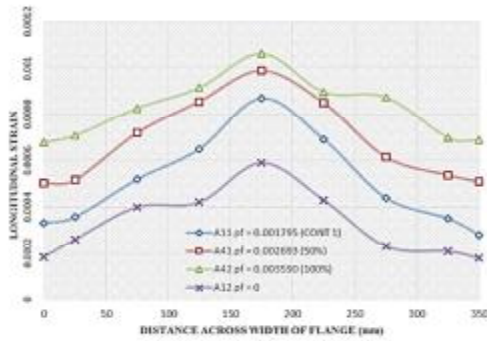


Figure (12) Flange top surface strain distribution at mid span and crack loading for beams A11, A41, A42, A12

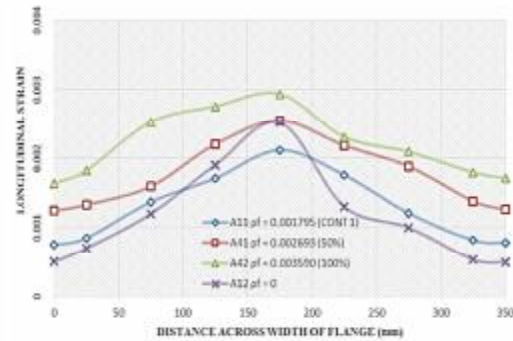


Figure (13) flange top surface strain distribution at mid span and ultimate loading for beams A11, A41, A42, A12

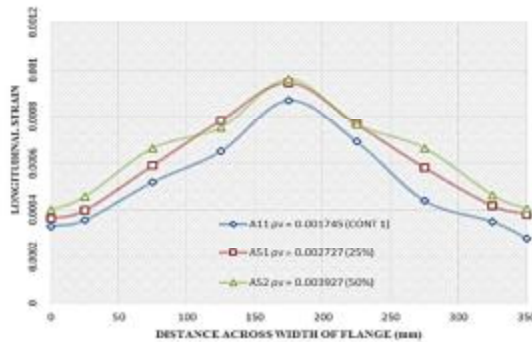


Figure (14) Flange top surface strain distribution at mid span and crack loading for beams A11, A51, A52

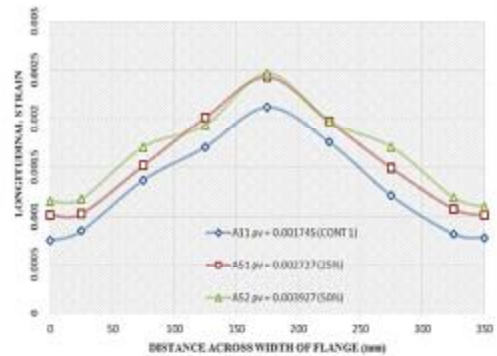


Figure (15) Flange top surface strain distribution at mid span and ultimate loading for beams A11, A51, A52

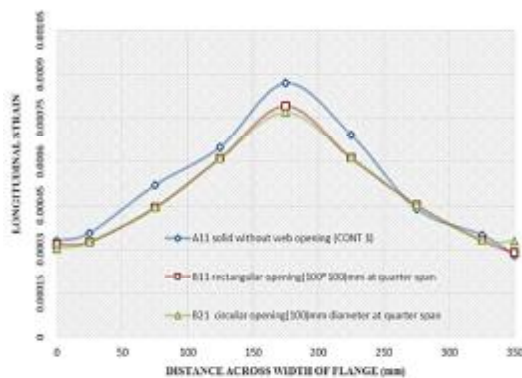


Figure (16) Flange top surface strain distribution at mid span in crack loading for beams A11, B11, B21

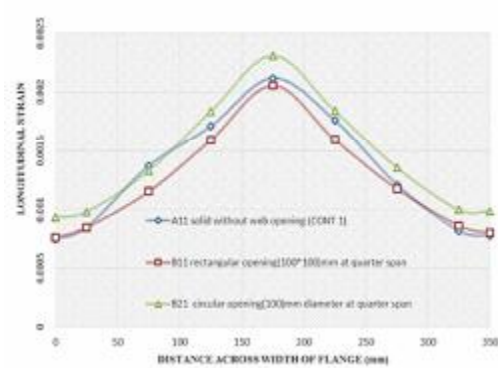


Figure (17) Flange top surface strain distribution at mid span in ultimate loading for beams A11, B11, B21

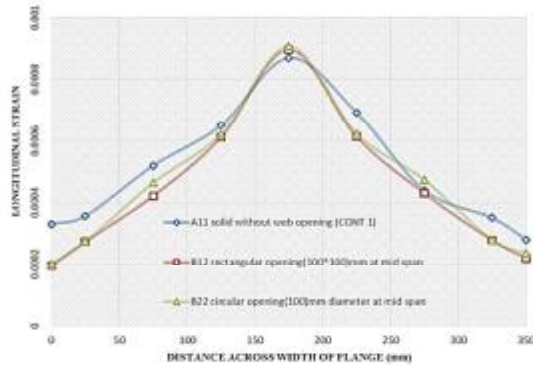


Figure (18) Flange top surface strain distribution at mid span and crack loading for beams A11,B12,B22

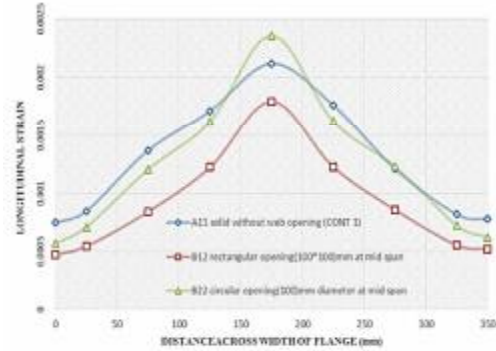


Figure (19) Flange top surface strain distribution at mid span and ultimate loading for beams A11,B12,B22

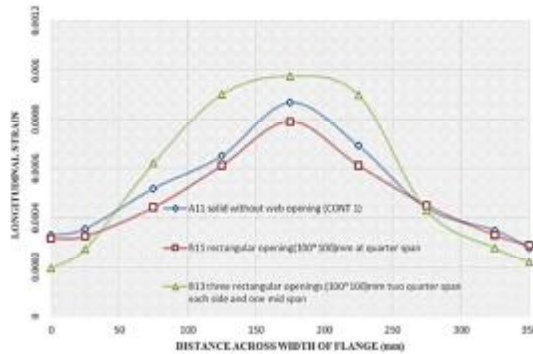


Figure (20) Flange top surface strain distribution at mid span and crack loading for beams A11,B11,B13

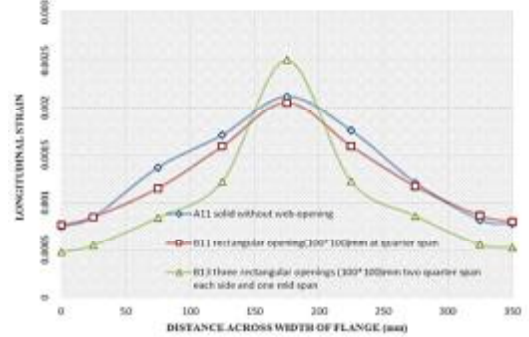


Figure (21) Flange top surface strain distribution at mid span and ultimate loading for beams A11,B11,B13

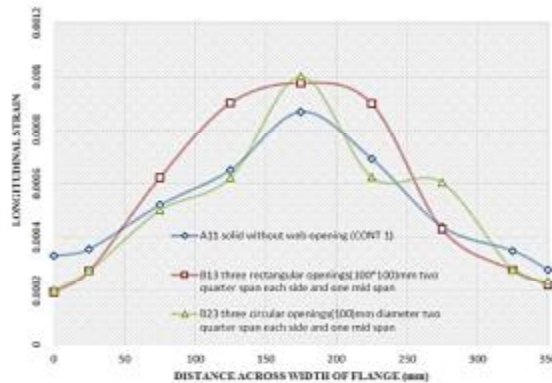


Figure (22) Flange top surface strain distribution at mid span and crack loading for beams A11,B13,B23

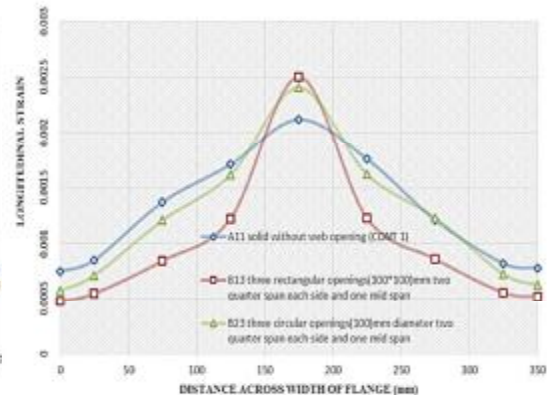


Figure (23) Flange top surface strain distribution at mid span and ultimate loading for beams A11,B13,B23

Table (2) Results of experimental work

GROUP	Beams	Sup group	L_n (m)	b_w (mm)	b_f (mm)	h_f (mm)	h (mm)	P_{cr} kN	P_u kN	P_{cr}/P_u	b_e (mm)	b_e/b_f	Type Failure	notes
Group A Without Openings	A1	A11	1.5	180	350	50	350	155	420	0.370	212	0.61	Flexure	REF1
		A12	1.5	180	350	50	350	150	400	0.375	183	0.53	Flexure	REF2
	A2	A21	1.5	180	350	50	350	160	450	0.355	224	0.64	Flexure	EFF. OF f_c
		A22	1.5	180	350	50	350	180	460	0.390	242	0.69	Flexure	
	A3	A31	1.5	180	350	50	350	160	450	0.355	230	0.66	Flexure	EFF. OF P_v
		A32	1.5	180	350	50	350	165	450	0.366	241	0.69	Flexure	
	A4	A41	1.5	180	350	50	350	160	410	0.390	225	0.65	Flexure	EFF. OF P_t
		A42	1.5	180	350	50	350	160	415	0.385	248	0.71	Flexure	
	A5	A51	1.5	180	350	50	350	165	420	0.393	217	0.62	Flexure	EFF. OF P_v
		A52	1.5	180	350	50	350	165	425	0.388	222	0.64	Flexure	
Group B With Openings	B1	B11	1.5	180	350	50	350	120	300	0.400	204	0.59	Flexure	EFF. OF NO. OF OPENING
		B12	1.5	180	350	50	350	115	280	0.411	182	0.52	Flexure	
	B2	B21	1.5	180	350	50	350	130	350	0.371	208	0.60	Flexure	EFF. OF SHAPE OF OPENING
		B22	1.5	180	350	50	350	130	310	0.419	185	0.53	Flexure	
	B3	B31	1.5	180	350	50	350	80	150	0.533	Failure	-	Shear	SIZE OPENING
		B32	1.5	180	350	50	350	60	180	0.333	Failure	-	Shear	

b_w = width of web
 b_f = width of flange
 h_f = thickness of flange

h = total depth of beam.
 P_{cr} = cracking load.
 P_u = ultimate load.

b_e = effective width of flange.
 b_f = real width flange.

CONCLUSIONS

1. For all the beams tested the failure is of flexure type except beams B31, B32 fail in shear type, the flexural behavior taken the mid span crushing in all beams except the beams with web opening have a type failure 45 degree inclined failure plane.
2. It was found when increased the concrete compressive strength leads to increase the elasticity behavior for beam, eventually raised the strain distribution along the flange then the effective width increased by 9.1%, 13.64% for 24Mpa, 30Mpa respectively.
3. Steel ratio for longitudinal tension bars increased the resistance and strain distribution for the beam more than shear reinforcement by 10.1%, 13.3% for 25%, 50% of amount the steel respectively, but the flange reinforcement increased the shear lag by 7.6%, 18.2% for 50%, 100% of amount the steel respectively.
4. Web opening location is the most critical factor which play an important role in the determination of the effective flange width.
5. Introducing central span web opening causes a maximum decrease in the effective width of about 48%, whereas a maximum decrease of about 40% is observed due to presence of quarter span web opening.
6. If the size of opening more than 1/3 depth of beam, the failure happened suddenly without indication.

REFERENCES.

- [1]. Mansur, M.A "Design of Reinforced Concrete Beams with Web Opening", 6th Asia-Pacific Structural Engineering and Construction Conference 6 Sep. 2006, Kuala Lumpur, Malaysia.
- [2]. Al-Sherrawi M.H.M and Fadhil G.A "Effect of stiffeners on shear lag in steel box girder" Alkharizmi Engineering Journal Vol.8, No.2, PP63-76
- [3]. Kucukarslan S. and Utku M., "A finite Element Study on the Effective width of flanged section", M.Sc. thesis July 2010, Middle East technical university.
- [4]. Sedlacek, G. and Bild, S., "A Simplified Method for the Determination of the Effective Width Due to Shear Lag Effects" Journal of Construction and Steel Research, Vol. 24, pp.155-182. April 1992.
- [5]. Yew-Chaye Loo and Tjitra D. Sutandi, "Effective flange width formulas for T-beams", Concrete International 1986, ACI Journal.
- [6]. M. Utku and A. Ayger, "Investigation of Effective Flange Width Formulas for T-Beams" Six International conference on computational structures technology, Stirling, Scotland 2002.
- [7]. Qin X. X. and Liu H. B. and Wang S. J. and Yan Z. H. "Simplistic Analysis of the Shear Lag Phenomenon in a T-Beam", the Journal of Engineering Mechanics, ASCE 2014, ISSN 0733-9399/04014157(15).
- [8]. Neville, A. M., "Properties of Concrete" Second Edition, Pitman Publishing Company Limited, London, 1987.
- [9]. Qi-gen Song, Alexander C. Scordelis, "Shear-Lag Analysis of T-, I- and box beams", J. Struct. Eng 1990. 116:1290-1305 ASCE.